JOURNAL OF Materials CHEMISTRY

Preparation and characterization of iron-encapsulating carbon nanotubes and nanoparticles

Suwen Liu,†[a] Xianghai Tang,[a] Yizhak Mastai,[b] Israel Felner[c] and Aharon Gedanken*[a]

[a]*Department of Chemistry, Bar-Ilan University, Ramat-Gan 52900, Israel. E-mail: gedanken@mail.biu.ac.il*
[b]*Department of Materials and Interfaces, Weizmann Institute of Science, Rehovot 76100, Israel*
[c]*Racah Institute of Physics, Hebrew University, Jerusalem 91904, Israel*

Received 19th June 2000, Accepted 25th July 2000
First published as an Advance Article on the web 14th September 2000

Iron-filled carbon nanostructures have been synthesized *via* a simple catalytic process, using $Fe(CO)_5$ as the source of both iron and carbon. The iron-containing materials can be separated from the products using a permanent magnet. The nanotubes have dimensions of several hundred nanometers in length and 10–20 nm in width. The fabrication of cup-like and centipede-like carbon nanostructures is reported for the first time. In addition, some large fractured carbon cages with an average diameter of 200 nm were also observed in the products. XRD measurements revealed that the encapsulated iron nanoparticles had a bcc structure. The magnetic properties of the products were evaluated by conducting dc magnetic measurements. XPS and TGA were also employed to characterize the products.

Introduction

Metallofullerenes, especially metal-filled carbon nanotubes, have been attracting intense scrutiny in recent years owing to their unique electronic, magnetic and nonlinear optical properties.[1] It has been suggested that these materials might find important applications in diverse areas, such as magnetic data storage, xerography and magnetic resonance imaging.[2] While the metal particles show quantum effects as their dimension decreases to the nanoscale, the carbon shells isolate the metal particles from each other, as well as from the outside environment. This protection also prevents the oxidation of the metallic particles. In addition, the lubricating properties of the graphite coating might be helpful in magnetic recording applications and reinforce material durability.[3,4] So far, various approaches, either *via* arc discharge[5–7] or post chemical treatments,[8,9] have been developed for encaging materials in carbon nanotubes and nanocapsules. However, in addition to the complicated procedures involved, these methods are confined to a limited range of metals or produce products in low yields. Therefore, it is of particular importance to establish new methods for the fabrication of such materials.

It has been demonstrated that transition metals are efficient catalysts for the fabrication of single- and multi-walled carbon nanotubes.[10–13] Thermolysis of hydrocarbons in the presence of organometallic complexes (*e.g.* metallocenes) has been reported to yield graphitic nanotubes.[14–16] Some of the as-prepared carbon nanotubes and nanocapsules were filled with metal particles; however, their hollow analogs were usually predominant and the composition, as well as magnetic properties, of the former were seldom studied. Rao *et al.* found that vapor-phase pyrolysis of $Fe(CO)_5$ in a gas flow containing Ar, H_2 and another carbon source (CO or C_6H_6) yielded iron-filled or hollow carbon nanotubes.[14b] More recently, Grobert *et al.* described a way to generate films of aligned carbon nanotubes filled with iron nanowires by annealing C_{60} in the presence of ferrocene.[17] Our previous work revealed that cobalt-filled carbon nanotubes and nanoflasks can be successfully fabricated by employing $Co(CO)_3NO$ as a precursor.[18] Unfortunately, no carbon nanotubes have, thus far, been obtained by thermolysis of $Fe(CO)_5$ alone.

In this paper, we report a very simple *in situ* method which yields iron-encapsulating carbon nanotubes and nanoparticles by employing $Fe(CO)_5$ as a precursor. This thermolysis feedstock not only acts as a source of carbon, but also gives rise to small metal clusters or particles which further catalyze the formation of the carbon nanotubes. The outer diameter of the nanotubes is 10–20 nm. The yield of iron-filled graphitic nanotubes and nanocapsules in our experiments was *ca.* 5% by mass. We report for the first time the preparation of cup-like and centipede-like carbon nanostructures. Moreover, a kind of large, fractured carbon cage with an average diameter of 200 nm is also fabricated.

Experimental

The synthesis was carried out in a 2 mL closed vessel cell, which was assembled from stainless steel Swagelok parts. A 3/8″ union part was capped from one side by a standard plug. In a typical synthesis, 0.5 g of magnesium powder and 0.5 mL of $Fe(CO)_5$ were placed in a cell at room temperature, after which the vessel was tightly closed immediately. The reactor was heated at 36 K min^{-1} to the desired temperature (*i.e.* 900, 1000 or 1100 °C) and was kept at this temperature for 3.0 h. The reaction took place under autogeneous pressure. After allowing it to cool naturally to ambient temperature, the vessel was found to be unpressurised. Two different kinds of products were obtained: a black, soft powder-like solid was found attached to the container's wall, especially near the cap; another kind of powder, which formed at the bottom of the vessel, appeared gray and hard. The powders were mixed and treated with 50 mL of 8 M HCl for 1.0 h at 70 °C and treated again overnight at room temperature. Finally, a black, soot-like mixture was obtained after filtering and rinsing. The powder of iron-containing moieties from the mixture was

†Also at: Department of Applied Chemistry, University of Science and Technology of China, Hefei, Anhui 230026, P. R. China.

 DOI: 10.1039/b004901h

This journal is © The Royal Society of Chemistry 2000

further enriched by the attraction of the magnetic particles to a permanent magnet.

Transmission electron microscopy (TEM) was performed on a JEOL JEM-1220 at 80 kV and high-resolution transmission electron microscopy (HRTEM) on a Phillips CM-120 at 120 kV. Specimens for TEM and HRTEM observations were sonicated in ethanol for 10 min and then loaded onto copper grids (200 mesh). X-Ray photoelectron spectroscopy (XPS) was recorded using a KRATOS ANALYTICAL AXIS HIS 160 ULTRA. X-Ray diffraction (XRD) patterns were taken with a Rigaku X-ray diffractometer (Model-2028, Cu-Kα radiation, 20 kV). Thermogravimetric–mass spectrometric analyses (TGA–MS) were carried out on a Mettler Toledo TGA/SDTA 851^e (equipped with a Balzers Thermostar GSD 300T3 unit) with and without an applied magnetic field (10 K min^{-1}, N_2 40 mL min^{-1}). Dc magnetic measurements in the range 5–300 K were conducted using a Quantum Design superconducting quantum interference device (SQUID) magnetometer.

Results and discussion

XRD

The XRD patterns of as-prepared samples obtained at 1100 °C are presented in Fig. 1, indicating that the black powder and the gray product differ in composition. The main peaks in Fig. 1a (black powder) can be indexed solely to bcc Fe, while those in Fig. 1b (gray powder) can be indexed to bcc Fe (JCPDS 6-696) and fcc MgO (JCPDS 30-794). After treating the powders together with concentrated HCl (8 M), MgO and most of the metallic iron were dissolved. This led to XRD patterns in which graphite became the dominant feature, iron was detected only as a weak signal and the MgO peaks were completely absent. Fig. 2 shows the XRD patterns of the HCl-treated samples prepared at various temperatures. Obviously, the higher temperature favors better crystallization of the graphite. Based on the XRD analyses, the following mechanism is proposed. In the first step, $Fe(CO)_5$ decomposes into Fe and CO and the iron atoms cluster together to form highly active nanoparticles. Subsequently, CO reacts with Mg to yield MgO and carbon. The reactions are as follows:

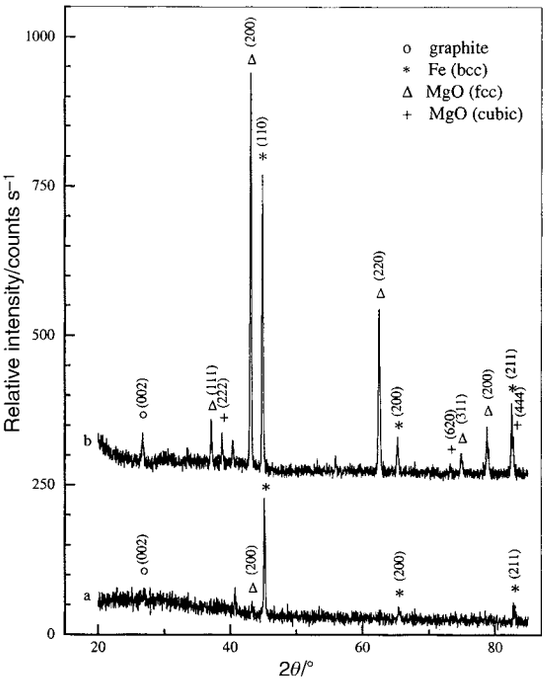

Fig. 1 XRD patterns of as-prepared (a) black and (b) gray powders obtained at 1100 °C.

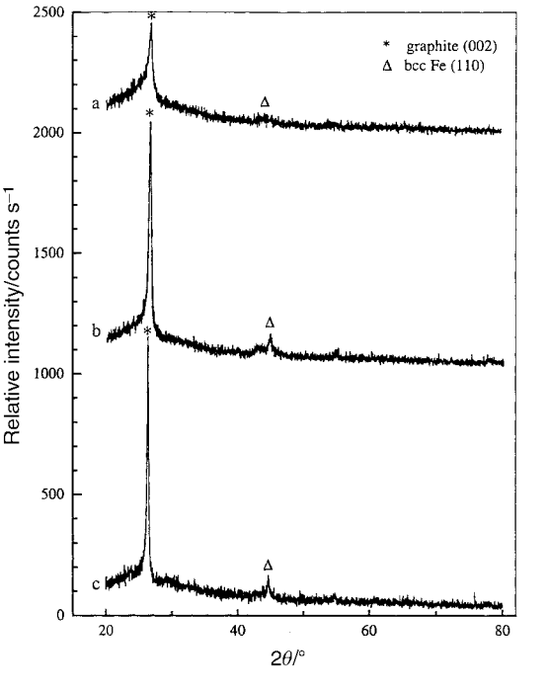

Fig. 2 XRD patterns of HCl-treated samples prepared at (a) 900, (b) 1000 and (c) 1100 °C.

$$Fe(CO)_5(g) \rightarrow Fe(s) + 5CO(g) \quad (1)$$

$$CO(g) + Mg(l) \rightarrow MgO(s) + C(s) \quad (2)$$

During the reduction of CO, the iron particles act as catalysts to orient the fabrication of nanotubes and nanoparticles with the *in situ* generated carbon. They are probably also important for the growth of cup-shaped fractured carbon cages (*vide infra*). Meanwhile, part of the metallic iron produced by the *in situ* thermolysis of $Fe(CO)_5$ is encapsulated within the carbon shells. Those iron particles not isolated by the graphitic shells are removed by the HCl treatment. The XRD patterns shown in Fig. 2 demonstrate that the samples contain small amounts of bcc Fe, even after prolonged treatment with concentrated HCl. This implies that iron is encapsulated within the carbon shells.

TEM

A typical TEM image (Fig. 3a) of the HCl-treated product shows nanotubes filled with spheroidal iron nanoparticles at the tips. Some iron-filled carbon nanoparticles were also observed by TEM. The nanotube dimensions are several hundred nanometers in length and 10–20 nm in diameter, while the quasi-spheroidal iron-filled carbon nanoparticles have external diameters ranging between 20 and 80 nm. Usually, the meandering nanotubes intertwist. Fig. 3b shows a HRTEM image of an iron-encapsulating nanoparticle with *ca.* 7 graphitic layers on the outside. Fig. 3c shows an iron nanoparticle at the tip of a carbon nanotube. The non-magnetic residues remaining after the removal of the iron-containing material with a permanent magnet were also analyzed by TEM. They revealed hollow carbon nanotubes and large cup-shaped fractured cages (Fig. 4). The cross-section of the fractured cages is approximately 100–200 nm long and 100 nm wide. Some fractured carbon cages packed in chains were also found, as shown in the upper part of Fig. 5. These cup-shaped carbon materials are somewhat similar to those formed by arc evaporation,[19,20] but the latter are much more slender (*ca.* 30 nm wide and >200 nm long). To date, no such large cup-shaped carbon nanostructures have been

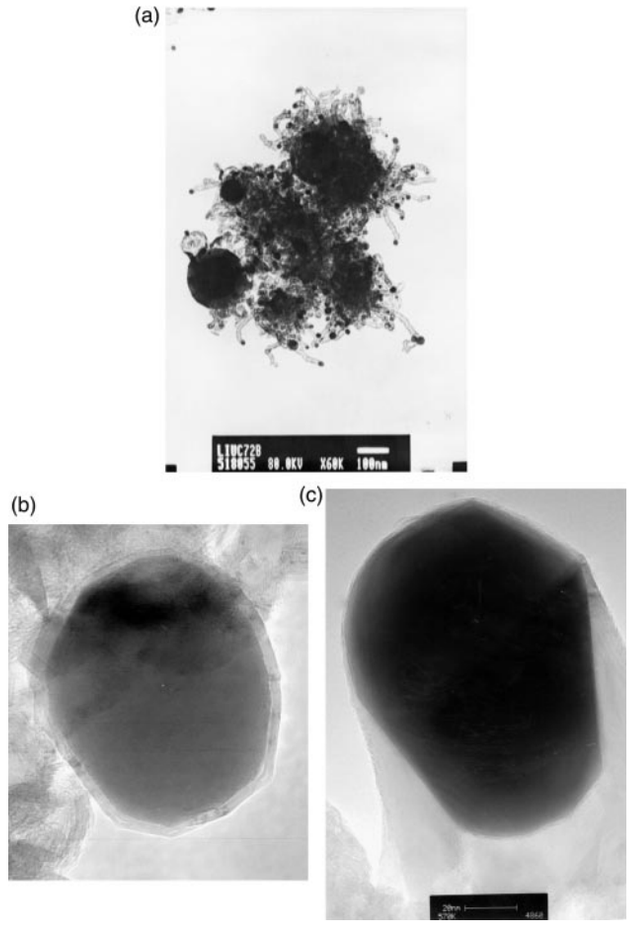

Fig. 3 (a) A typical TEM image of iron-encapsulating carbon nanotubes. (b) A HRTEM image of an iron nanoparticle encapsulated in a quasi-spheroid. (c) A HRTEM image of an iron nanocrystal located at the tip of a carbon nanotube.

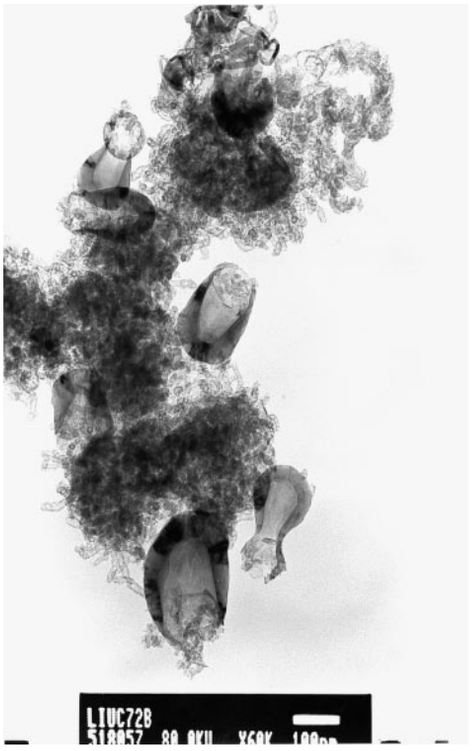

Fig. 4 A TEM image of the non-magnetic residues of a HCl-treated sample after removal of the iron-containing material with a magnet.

Fig. 5 A TEM image of a carbon nanoflask and a chain consisting of hollow graphitic cages.

reported. We suggest that these cages might have been filled with iron or other materials (*e.g.* MgO) in their cores and, upon the HCl treatment, they became empty. Unlike our previous results with $Co(CO)_3NO$,[18] we failed in the present work to obtain long, straight, thick-walled carbon nanotubes filled with metallic nanowires. We have obtained, on the other hand, mainly short, tortuous, thin-walled nanotubes. We speculate that these nanotubes are formed during the early stages of the reaction. The quality of the tubes obtained from $Fe(CO)_5$ at 1100 °C is not as good as those obtained at 900 °C in the synthesis which employs $Co(CO)_3NO$. A few iron-filled nanoflasks were found in the products. Also of interest is the observation of the long, ribbon-like structure of a flattened nanotube[21] stretching from the neck of a flask (Fig. 5). However, the content of such nanoflasks in the products is much less than that in the case of $Co(CO)_3NO$. In addition, some strangely structured carbon materials, which are centipede-like and assembled with graphitic fragments, were also found in the TEM images and are shown in Fig. 6. The structures are probably the early stages of carbon nanotubes which are similar to those obtained using $Co(CO)_3NO$ as a precursor. These phenomena imply that cobalt is a more effective catalyst than iron for the fabrication of carbon nanotubes according to eqn. 2. Interestingly, selected area electron diffraction (SAED) analysis did not detect any iron carbide species, such as FeC_3, FeC, *etc.* This is in accord with the XRD results. Indeed, a relatively low temperature does not favor the formation of carbides, thus the sample has a simple composition. This is one of the advantages of our chemical, catalytic method, as carbides are usually formed as by-products in the arc discharge approaches.[5–7]

XPS and TGA

The XPS spectrum recorded on the HCl-treated sample identified only pure carbon (*i.e.*, no Fe signal). This is inconsistent with the TEM results, indicating that metallic iron is enclosed within the carbon nanotubes or shielded by the graphite capsules. When the sample was bombarded with an Ar ion gun, the iron signal appeared. Fig. 7 shows the iron content as a function of etching time of a HCl-treated sample prepared at 1100 °C. The iron content in the product is about 1.1% (atomic ratio). The TGA results for this sample measured with

Fig. 6 A TEM image of centipede-like carbon.

and without an applied magnetic field are depicted in Fig. 8. In the case in which there was no applied magnetic field (Fig. 8a), a rapid drop in mass was observed between 730–830 °C. The mass spectrometric analysis revealed that the effluent at temperatures above 720 °C contained FeO_2.[22] However, when a magnet was placed above the sample chamber, there was only a slight drop in mass above 650 °C (Fig. 8b). This difference can be attributed to the effect of the magnetic field on FeO_2. When a magnetic field was applied, most of the FeO_2 was attracted onto the lid of the crucible and kept there, while, without an applied magnetic field, the magnetic species were carried away by the flow.

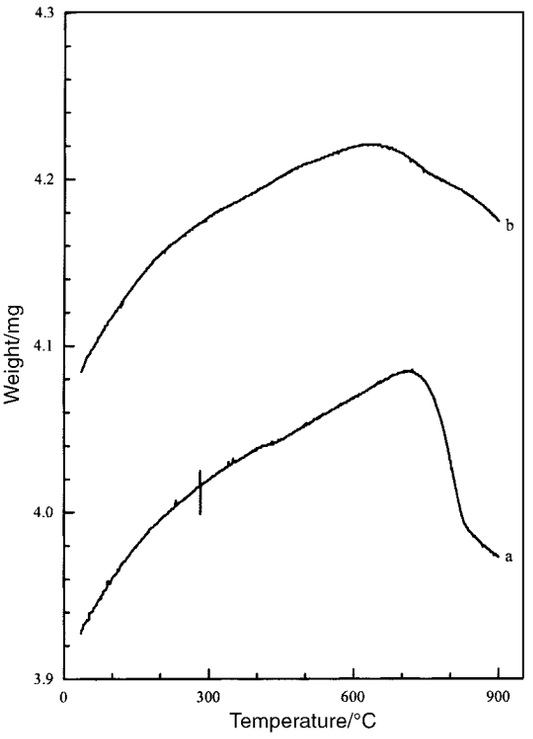

Fig. 8 TGA curves measured (a) without and (b) with an applied magnetic field for the sample prepared at 1100 °C after treatment with HCl.

Magnetic properties

Dc magnetic measurements of a sample in the range 5–300 K (up to 50 kOe) were performed and are presented in Fig. 9. The magnetization, $M(H)$, has been evaluated at various temperatures. As shown in Fig. 9, for the HCl-treated sample prepared at 1100 °C, the $M(H)$ curves at 5 and 295 K are strongly dependent on the field up to about 10 kOe, until the typical saturation for ferromagnetic substances was reached. No hysteresis behavior was observed. Due to the low contribution

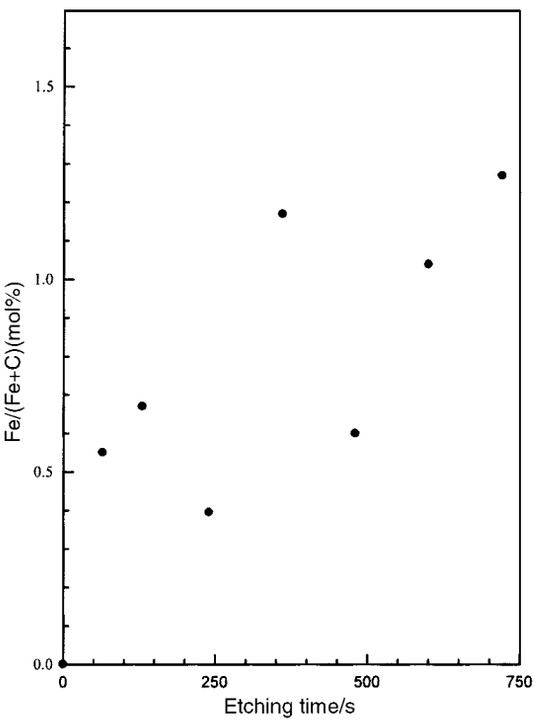

Fig. 7 XPS results: iron content *vs.* etching time of the sample prepared at 1100 °C after treatment with HCl.

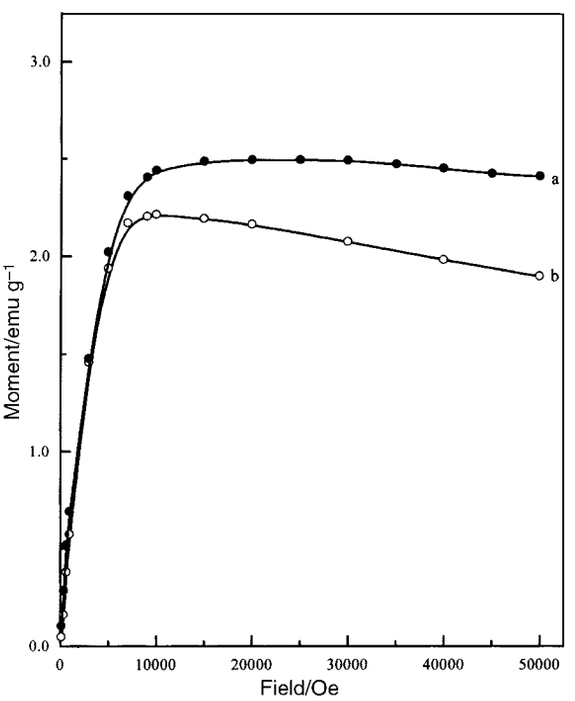

Fig. 9 The magnetization at (a) 5 and (b) 295 K for the sample prepared at 1100 °C after treatment with HCl.

of carbon, it is assumed that the $M(H)$ curves mainly show the magnetic contribution of iron encaged within the carbon shells. The saturation moment (σ_s) of pure iron metal is about 220 emu g^{-1}. Therefore, the magnetization value at 5 K (σ_s = 2.5 emu g^{-1}) corresponds to 1.13% Fe in weight, assuming that the iron in the product behaves similarly to pure Fe and not taking into account the size effect. At ambient temperature, the saturation moment decreases by only 20%, indicating a high magnetic transition temperature for this system. Using the same logic, we estimate that the sample prepared at 900 °C contains only 0.40% Fe by mass. Due to the low iron concentration, attempts to carry out Mössbauer measurements on these samples were unsuccessful.

Acknowledgements

Dr Suwen Liu and Dr Xianghai Tang thank the Fred and Barbara Kort Sino-Israel Postdoctoral Fellowships Foundation for financial support and the China Scholarship Council for its support. A. Gedanken and I. Felner thank the Ministry of Science for an Infrastructure Strategic Grant. A. Gedanken thanks the German Ministry of Education and Research, through the Deutsche–Israeli Program (DIP), and the NEDO International Joint Research Grant for their financial support. The authors would like to thank Dr Shifra Hochberg for editorial assistance.

References

1 R. S. Ruoff, *Nature*, 1994, **372**, 731.
2 S. A. Majetich, J. O. Artman, M. E. McHenry, N. T. Nuhfer and S. W. Staley, *Phys. Rev. B*, 1993, **48**, 16845.
3 P. J. F. Harris, *Carbon Nanotubes and Related Structure*, Cambridge University Press, Cambridge, 1999, pp. 164–185.
4 Y. Saito, T. Yoshikava, M. Okuda, M. Ohkohchi, Y. Ando, A. Kasuya and Y. Nishina, *Chem. Phys. Lett.*, 1993, **209**, 72; Y. Saito, T. Yoshikava, M. Okuda, N. Fujimoto, S. Yamamuro, K. Wakoh, K. Sumiyama, K. Suzuki, A. Kasuya and Y. Nishina, *Chem. Phys. Lett.*, 1993, **212**, 379; Y. Saito, T. Yoshikawa, M. Okuda, N. Fujimoto, S. Yamamuro, K. Wakoh, K. Sumiyama, K. Suzuki, A. Kasuya and Y. Nishina, *J Appl. Phys.*, 1994, **75**, 134.
5 S. Seraphin, D. Zhou, J. Jiao, J. C. Withers and R. Loufty, *Nature*, 1993, **362**, 503.
6 C. Guerret-Piecourt, Y. Le Bouar, A. Loiseau and H. Pascard, *Nature*, 1994, **372**, 761.
7 E. Dujardin, T. W. Ebbesen, H. Hiura and K. Tanigaki, *Science*, 1994, **265**, 1850.
8 P. M. Ajayan and S. Iijima, *Nature*, 1993, **361**, 333.
9 S. C. Tsang, Y. K. Chen, P. J. F. Harris and M. L. H. Green, *Nature*, 1994, **372**, 159.
10 W. Z. Li, S. S. Xie, L. X. Qian, B. H. Chang, B. S. Zou, W. Y. Zhou, R. A. Zhao and G. Wang, *Science*, 1996, **274**, 1701.
11 C. R. Martin, *Science*, 1994, **266**, 1961.
12 A. Thess, R. Lee, P. Nikolaev, H. Dai, P. Petit, J. Robert, C. Xu, Y. H. Lee, S. G. Kim, D. T. Colbert, G. Scuseria, D. Tomanek, J. E. Fischer and R. E. Smalley, *Science*, 1996, **273**, 483.
13 H. Dai, A. G. Rinzler, P. Nikolaev, A. Thess, D. T. Colbert and R. E. Smalley, *Chem. Phys. Lett.*, 1996, **260**, 471.
14 (*a*) C. N. R. Rao, R. Sen, B. C. Satishkumar and A. Govindaraj, *Chem. Commun.*, 1998, 1525; (*b*) R. Sen, A. Govindaraj and C. N. R. Rao, *Chem. Mater.*, 1997, **9**, 2078; (*c*) R. Sen, A. Govindaraj and C. N. R. Rao, *Chem. Phys. Lett.*, 1997, **267**, 276; (*d*) B. C. Satishkumar, A. Govindaraj, R. Sen and C. N. R. Rao, *Chem. Phys. Lett.*, 1998, **293**, 47; (*e*) K. Bladh, L. K. L. Falk and F. Rohmund, *Appl. Phys. A*, 2000, **70**, 317.
15 S. L. Huang, L. Dai and A. W. H. Mau, *J. Mater. Chem.*, 1999, **9**, 1221.
16 Q. T. Le, M. C. Schouler, J. Garden and P. Gadelle, *Carbon*, 1999, **37**, 505.
17 N. Grobert, W. K. Hsu, Y. Q. Zhu, J. P. Hare, H. W. Kroto, M. Terrones, H. Terrones, Ph. Redlich, M. Ruhle, R. Escudero and F. Morales, *Appl. Phys. Lett.*, 1999, **75**, 3363.
18 S. W. Liu, X. H. Tang, L. X. Yin, Y. Koltypin and A. Gedanken, *J. Mater. Chem.*, 2000, **10**, 1971.
19 C. H. Kiang, W. A. Goddard III, R. Beyers, J. R. Salem and D. S. Bethune, *J. Phys. Chem.*, 1994, **98**, 6612.
20 Y. Saito and T. Yoshikawa, *J. Cryst. Growth*, 1993, **134**, 154; Y. Saito, T. Yoshikawa, M. Okuda, N. Fujimoto, K. Sumiyama, K. Suzuki, A. Kasuya and Y. Nishina, *J. Phys. Chem. Solids*, 1993, **54**, 1849.
21 N. G. Chopra, L. X. Benedict, V. H. Crespi, M. L. Cohen, S. G. Louie and A. Zettl, *Nature*, 1995, **377**, 135.
22 D. Schröder, A. Fiedler, J. Schwarz and H. Schwarz, *Inorg. Chem.*, 1994, **33**, 5094; D. Schröder, A. Fiedler, W. A. Herrmann and H. Schwarz, *Angew. Chem., Int. Ed. Engl.*, 1995, **34**, 2517.